

Neutron reflectometry as a tool to study magnetism (invited)

G. P. Felcher

Material Science Division, Argonne National Laboratory, Argonne, Illinois 60439

Polarized-neutron specular reflectometry (PNR) was developed in the 1980's as a means of measuring magnetic depth profiles in flat films. Starting from simple profiles, and gradually solving structures of greater complexity, PNR has been used to observe or clarify a variety of magnetic phenomena. It has been used to measure the absolute magnetization of films of thickness not exceeding a few atomic planes, the penetration of magnetic fields in micron-thick superconductors, and the detailed magnetic coupling across nonmagnetic spacers in multilayers and superlattices. The development of new scattering techniques promises to enable the characterization of lateral magnetic structures. Retaining the depth sensitivity of specular reflectivity, off-specular reflectivity may be brought to resolve in-plane structures over nanometer to micron length scales. © 2000 American Institute of Physics. [S0021-8979(00)15508-2]

I. REFLECTOMETRY

Polarized neutron reflectometry (PNR) was devised in the mid-1980's as an analytic tool to measure the magnetic depth profile of thin films or in proximity of surfaces and interfaces. Its deployment was paralleled by the evolution of techniques capable of producing reliable magnetic films with novel magnetic properties.¹ Neutron reflectivity is an optical technique:^{2,3} the interaction of neutrons with the medium through which they propagate is described by a potential whose magnitude is related simply to the scattering length density of the nuclei and the magnetic induction B in the material:

$$V_{\text{eff}} = V_n + V_m = \frac{2\pi\hbar^2}{m} bN + \mathbf{B} \cdot \hat{\mathbf{s}}, \quad (1)$$

where b is the mean of the scattering lengths over the N atoms occupying a unit volume and s is the neutron spin. The trajectory of the neutron in this potential is obtained by solving the Schrödinger equation. If V_{eff} is function only of the depth from the surface (as in a stratified medium) only the z component of the motion perpendicular to the surface is affected by it: the motion in the plane x, y (parallel to the surface) is that of a free particle.

As shown in Fig. 1, a beam of neutrons is specularly reflected from a flat, laterally homogeneous object. The intensity of the reflected beam, recorded at different neutron wavelengths and angles of incidence, permits an evaluation of the chemical and magnetic depth profile. In vacuum the component of the neutron momentum perpendicular to the

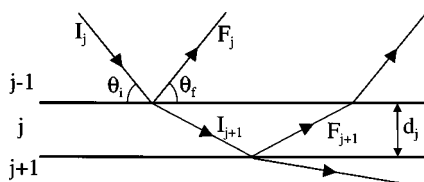


FIG. 1. Scheme of reflection and refraction from a couple of flat layers perpendicular to z .

surface is $k_{zv} = 2\pi \sin \theta / \lambda$, where θ is the angle of incidence on the surface and λ the neutron wavelength.

When Eq. (1) contains only a nuclear potential, in the medium the wavevector becomes

$$k_z = \sqrt{(k_{zv}^2 - 4\pi bN)}. \quad (2)$$

Reflection as well as refraction takes place at the surface; in a layered medium, the same can be said of any interface. The conditions of continuity of particles and their flux at the interface between layers j and $j+1$ yield the expression for the reflectance r_j :

$$r_j = \exp(-ik_{zj}d_j)(r_{j+1} + F_j)/(r_{j+1}F_j + 1), \quad (3)$$

where

$$F_j = (k_{zj+1} - k_{zj})/(k_{zj+1} + k_{zj}). \quad (4)$$

From such expressions reflectance can be calculated at the surface, r_s and the reflectivity $R = |r_s|^2$ which is the observable quantity. The wave vector transfer

$$q_z = k_{zf} - k_{zi} = 4\pi \sin \theta / \lambda, \quad (5)$$

provides a convenient metric for characterizing the specular reflection process. Since the momentum q_z is the quantum mechanical conjugate to position z , one can transform the depth profile of scattering material $b(z)$ into reflectivity $R(q_z)$. Equation (3) can be solved only iteratively. At large values of q_z both r_j and F_j are much less than 1. Neglecting higher order terms in the denominator, r_s reduces to a sum of F_j over all interfaces: this is the kinematical approximation. The expressions given above are valid as well when dealing with x-ray reflectivity: only the numerical values of the scattering length densities need to be changed.

Neutrons also interact with the magnetic induction fields \mathbf{B} in the material. Since the neutron is a spin-1/2 particle, there are two states of quantization with reference to an external magnetic field \mathbf{H} . When all neutrons are in one of these states they are polarized either parallel (+) or antiparallel (-) to \mathbf{H} . If the magnetic induction everywhere in the neutron path is parallel to H , neutrons remain polarized in

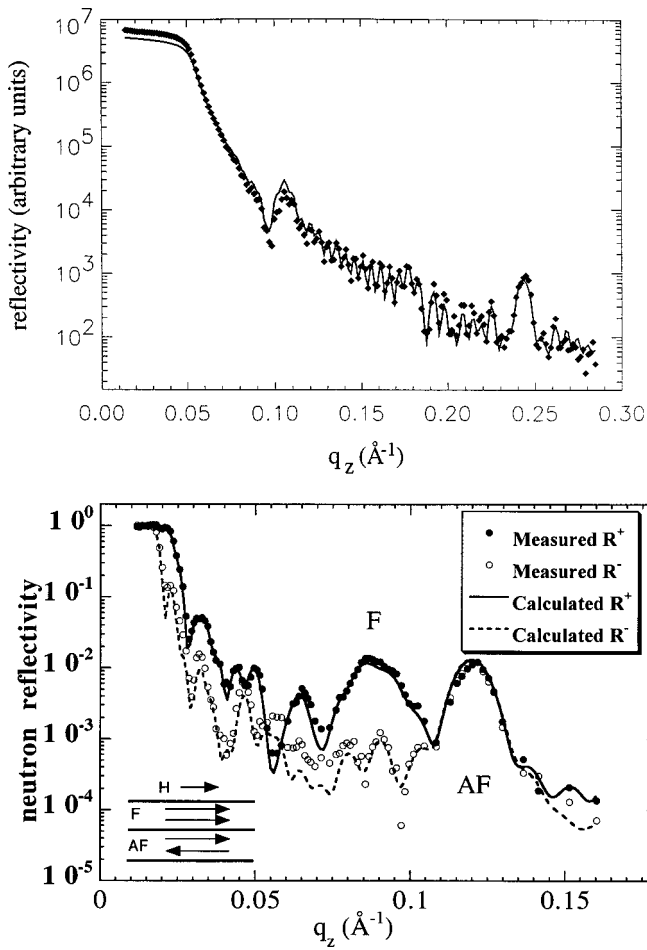


FIG. 2. Neutron and x-ray reflectivity from a double superlattice of Fe/Cr, composed of 5 layers of ferromagnetic [Fe (54 Å)/Cr (18 Å)] on top of 20 layers of AF [Fe (14 Å)/Cr (12 Å)]. The neutron reflectivities were calculated with parameters extracted from the x rays and the magnetization data (Ref. 4).

the original state, and see a potential $U^\pm = (\hbar^2/2m)Nb \pm \mu B$, where μ is the neutron magnetic moment. The magnetic medium is, in effect, birefringent.

To illustrate the notions introduced above (Fig. 2) presents the x-ray and neutron reflectivity from a “double superlattice” of Fe/Cr.⁴ The x-ray pattern extends over a range of q_z much larger than that of neutrons, thanks to the higher intensity of the source and also to the higher scattering density of the layers. The neutron reflectivity is strongly spin dependent, because of the relatively large scattering amplitude. The x-ray reflectivity was fitted by a chemical profile, and in turn this, together with information obtained from magnetization measurements, was used to calculate the PNR profiles without any fitting.

The problem of fitting PNR data has been found difficult to solve. Since the dynamic range is less extensive than for x-rays, approximate methods⁵ turn out to be less useful. A number of fitting routines have been proposed.⁶ However, the reflected intensity $R = |r|^2$ does not contain the phase information required for a unique determination of sample structure. There have been a number of recent advances in direct inversion of reflectivity data that, retain the phase of r , by means of the addition of two or three reference layers.^{7,8}

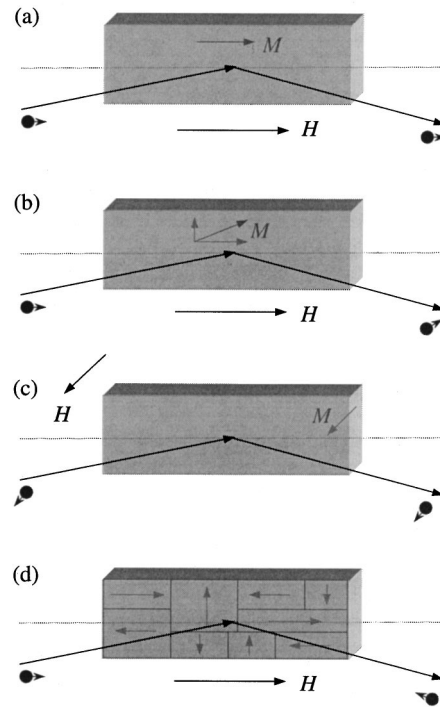


FIG. 3. Different spin-dependent process in the reflectivity. (a) With $B \parallel H$ the spin remains unaltered during reflection; (b) with $B \perp H$ in the film plane, the neutron processes around B (c) if B is perpendicular to the surface, $B = H$ regardless of z , hence there is no magnetic scattering (d) magnetic domains with different orientation of the magnetization quench, the polarization of the neutrons.

Figure 3 summarizes the behavior of the neutron spin during reflection for different magnetic systems. In all cases, neutrons are initially polarized along a magnetic field H and experience a magnetic induction B within the material. The difference is clear between the cases illustrated in Figs. 3(b) and 3(d). In the former case the reflected neutrons are still polarized, but in a direction different from the original one; in the latter case, the neutrons become partially depolarized. In all current experiments, only the projection along H of the polarization of the reflected neutrons is measured and cases (b) and (d) cannot be distinguished. Still, with such arrangement the experimental findings can be described in terms of four reflectivities: R^{++} , R^{--} , R^{+-} , and R^{-+} , where the first sign indicates the polarization state of the neutron before reflection and the second after reflection.

In some circumstances, the interpretation of the spin dependence of scattering is straightforward. This is the case of an AF Bragg diffraction peak due to a series of magnetic layers, of spacing d and magnetization M alternately magnetized in opposite direction but with orientation different from that of the quantizing field H . The AF Bragg diffraction peak in the reflection spectrum is centered at $q_z = 2\pi/d_{AF}$, with $d_{AE} = 2d$. The reflectivities, integrated over the width of the Bragg reflection, are proportional to

$$R^{\pm\pm} = M_{\parallel}^2; R^{\pm\mp} = M_{\perp}^2, \tag{6}$$

where M_{\parallel} and M_{\perp} are, respectively, the projections of the sublattice magnetization parallel and perpendicular to H . For other values of q_z this simple relationship does not hold. For

instance, it is easy to show that R^{+-} tends to decrease with q_z in the total reflection region, with the asymptotic behavior $R^{+-} \rightarrow 0$ when $q_z \rightarrow 0$. While the reflectivity can be easily calculated for any given magnetic structure,^{9,10} often the reverse path is not transparent, and the details of the noncolinear structure are obtained by model fitting.

A reflectometer is a simple instrument: a neutron beam of wavelength λ hits a sample surface at an angle θ and is reflected from the surface at the same angle θ . The instrument is practically a diffractometer with resolution sufficient to separate transmitted and reflected beams at values of q_z where the reflectivity becomes unitary. The reflectivity is solely a function of the momentum transfer along the z direction, and $q_z = 4\pi \sin \theta / \lambda$ can be spanned either by changing the wavelength, and keeping the angle of incidence fixed, or by changing the angle of incidence at fixed wavelength. Appropriate devices are added to polarize the incoming neutrons along an applied magnetic field or to analyze the polarization of the reflected beam. Reversal of the neutron spin is obtained by energizing flippers placed before and after the sample.⁴

II. RESEARCH ON MAGNETISM: A PARTIAL SURVEY

The goal of the first PNR experiment was to measure the London penetration depth λ_L in superconducting niobium.¹¹ The penetration depth characterizes completely the diamagnetism of a film for applied magnetic fields below H_{c1} , the field below which magnetic flux is expelled from the bulk of the material. Values of the penetration depth determined by PNR include conventional superconductors, like niobium,¹² lead,¹³ and high- T_c superconductor $\text{YBa}_2\text{Cu}_3\text{O}_{7-x}$, where the measurements point to a penetration depth of the order of 1400 Å,^{14,15} in good agreement with the results obtained by muon spin rotation. A distinguishing feature of PNR is the capability to verify if the magnetic field decays from the surface exponentially or with a more complex behavior. This issue is important when attempting to measure the magnetic depth profiles of type II superconductors in fields exceeding the critical value H_{c1} .

Above H_{c1} , an inhomogeneous state is created in type II superconductors, with the magnetic field penetrating along lines of fluxoids. For fields perpendicular to the surface, arrays of fluxoids have been observed with surface-sensitive techniques. With the field parallel to the surface the fluxoids may remain parallel to the surface and entirely submerged within the material. Up to now the presence of fluxoids in this geometry has been derived from careful measurements of the spin dependence of the specular reflectivity. If the fluxoids are pinned at random along the thickness z of the film their effect can be seen only close to the value of q_z for total reflection. However, a line of fluxoids located at the center of a superconducting film of thickness D gives rise to an spin dependence of the reflectivity extended to $q_z = 4\pi/D$.^{16,17} An array of Josephson fluxoids in a multilayer should exhibit a maximal spin dependence of the reflectivity at the Bragg reflections of the multilayer.¹⁸

Most of the research by PNR has been addressed to the magnetism of thin layers, either single or coupled to form

multilayers. For a film thickness of the order of 10 Å the magnetization of a ferromagnet is significantly altered from the bulk value in size, direction of magnetization, and even type of magnetic order. These new properties are the result of a complex set of circumstances, such as the incomplete quenching of the orbital moments, the stretching (or compressing) of the lattice on the substrate, and the transfer of electrons between magnetic film and substrate. Polarized neutron reflection has been used to determine the absolute value of the magnetic moment per atom in very thin films (five atomic planes) sandwiched between Ag on one side and Pd, Ag, Au, Cu, on the other side. At this thickness, an average moment per Fe atom has been found of $\sim 2.5 \mu_B$, against a bulk value of $2.2 \mu_B$.¹⁹ This result is in agreement with the 30% increase of the Fe moment predicted for the surface layer. In contrast, it was found that Ni in Cu/Ni/Cu sandwiches exhibits a decreased magnetization for films as thick as 100 Å, with a residual magnetization of $\sim 0.1 \mu_B/\text{Ni}$ at a nickel thickness of 30 Å.²⁰

First for a few selected pairs, then for a host of combinations of Fe, Co, Ni interleaved by most of the 3, 4, and 5d transition metals, it was found that the coupling between subsequent ferromagnetic layers oscillates from ferromagnetic (FM) to antiferromagnetic (AF) by varying the thickness of the nonmagnetic spacers. Magnetic fields ranging from several to a few thousand oersted saturate the magnetization of AF-coupled multilayers, with a corresponding large change of magnetoresistance. The basic magnetic structure predicted for the AF state is of type (+ - + -), a simple doubling of the chemical periodicity d . This structure has been confirmed directly by PNR first in multilayers of Fe/Cr (Ref. 21) and since then in a host of other multilayers. The basic PNR experiment consists of measuring the intensity of Bragg reflections at the values of $2 \sin \theta / \lambda$ equal to $1/d$ and $1/2d$: the first gives information on the ferromagnetic contribution of the average bilayer, the second on the AF contribution. Hydrogenation reversibly changes the band structure and metallic character of the components of a multilayer in a selective way, and by an amount controllable with the hydrogen pressure. Magnetically, the effect of hydrogenation is to switch reversibly between the AF- and FM-coupled states. In Nb/Fe and V/Fe superlattices, it has been shown^{22,23} that hydrogen enters solely in the Nb and V lattices and that the AF state is again characterized by a simple (+ - + -) sequence.

PNR has gradually been applied to unravel considerably more complex magnetic systems. In general, to determine the details of the magnetic profile of the repeat unit of a superlattice, a large q_z region needs to be explored. If the superlattice is composed of epitaxial layers, with the in-plane structure in registry, Bragg reflections appear at $q_z \sim 2 \text{ \AA}^{-1}$, corresponding to the mean atomic plane spacing a . Close to these lines, at $q_z = 2\pi[(1/a) \pm (1/d)]$, satellites appear due to the modulation of the superlattice spacing d with the atomic spacing a . By comparing the intensities of these satellites, it is possible in principle to determine the magnetization of the layer with a resolution of one atomic plane. Already in the 1980's extended range diffraction measurements on Gd/Y superlattices were used to test the presence of

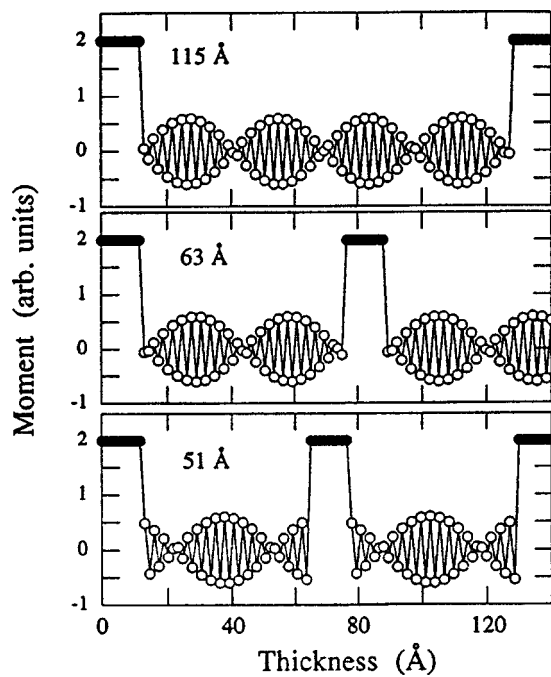


FIG. 4. Schematic representation of the magnetic moments for Fe and Cr layers in 115, 63, and 51 Å period samples. The moments were determined from the position and the intensities of the diffraction peaks around Cr (001), from Ref. 25.

magnetic dead layers at the interface.²⁴ More recent is the quest of the antiferromagnetic response of chromium in Fe/Cr superlattices. Bulk Cr orders magnetically, with an induced magnetic moment of less than $1 \mu_B$ modulated into an antiferromagnetic spin density wave (SDW). The SDW gives rise to magnetic satellites around the Cr(001) diffraction line. In Fe/Cr superlattices²⁵ it has been found that the SDW is modified, in period and phase, by the adjacent strong ferromagnetic layers (Fig. 4).

Analysis of the polarization state of reflected neutrons has been used in those cases, in which the direction of the magnetization was suspected of being depth dependent. Perhaps the case most discussed in recent years has been that of biquadratic exchange. Two ferromagnetic layers, separated by a spacer of thickness to provide only a very weak coupling, have been found to exhibit a 90° magnetization, thereby minimizing biquadratic terms $J \cdot M_1^2 M_2^2$ of the energy. Sustained research has been done by PNR to see if conformations of this kind persist in multilayers of Fe/Cr. The experimental pattern indicated the presence of both a FM Bragg reflection at $q_z = 2\pi/d$ and an AF one at half that value. From these $|M_{1\parallel}^1 + M_{2\parallel}^2|^2$, $|M_{1\perp}^1 + M_{2\perp}^2|^2$, $|M_{1\parallel}^1 - M_{2\parallel}^2|^2$, $|M_{1\perp}^1 - M_{2\perp}^2|^2$ were extracted separately [Eq. (6)] and the relative orientation of the moments in the average bilayer was reconstructed, assuming the system homogenous (not composed of ferromagnetic and antiferromagnetic domains). In general the angle between subsequent layers was found to be acute, in some cases approaching 90° .^{26,27}

In 1990 a model system was proposed²⁸ to describe the magnetic phases of tightly coupled multilayers, namely Gd/Fe. From the basic knowledge of the interaction between Gd and Fe on the atomic scale, individual layers of Gd and Fe

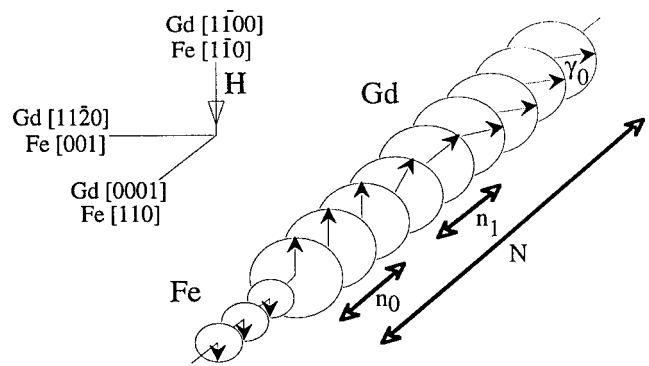


FIG. 5. Schematic representation of the moment configuration in a Gd/Fe bilayer showing the Gd twisted state (from Ref. 29).

were assumed to be ferrimagnetic with the net moment aligned toward a weak magnetic field. Increasing the field was predicted to cause a phase transition from the ferrimagnetic to a twisted configuration. The transition was broadened in a multilayer composed of a finite number of elements, in view of surface effects that cause the twist to be depth dependent. The detailed amount of predictions constituted quite an open challenge to the experimentalists, who were setup to confirm their applicability to real systems. However, the confirmation of the effect, by PNR measurements on Fe/Gd multilayers, was not direct: the intensity of Bragg reflections gives information on the magnetization of the average bilayer and thus does not address the problem of surface-induced transitions. This requires an analysis of the intensity reflected off the Bragg reflections, but for a multilayer this becomes quite a complex task. The most direct experimental evidence of a depth dependent twist of the magnetic moments was found in a single bilayer of Gd/Fe. At the contact point between the two layers the magnetization vectors of the gadolinium and iron layers were found to be oppositely aligned, and such an arrangement persists throughout the respective layers in zero field. However, when a magnetic field is applied the softer exchange interaction within the gadolinium layers gave rise to a twisted configuration (Fig. 5).²⁹

Fe/La multilayers³⁰ exhibit a fragile helical magnetic structure, stable in time, but permanently destroyed after application of a field of 100 Oe. In one of those rare cases in which PNR served as a primary diagnostic tool, such an effect turned out to result from imprinting during film deposition, rather than by interlayer coupling. Each layer was 30 Å thick, and during deposition the sample was rotated in an external field of 3 Oe, strong enough to magnetize the Fe layer being deposited but not sufficient to perturb the magnetization of the Fe layers already grown. As revealed by PNR, adjacent Fe layers formed a helical structure (Fig. 6) with a chirality and periodicity determined by the rotational direction and speed of the substrate and the rate of deposition.

III. OFF-SPECULAR SCATTERING

Until now we considered the reflectivity from a stack of infinite parallel layers with sharp boundaries (Fig. 1). Real

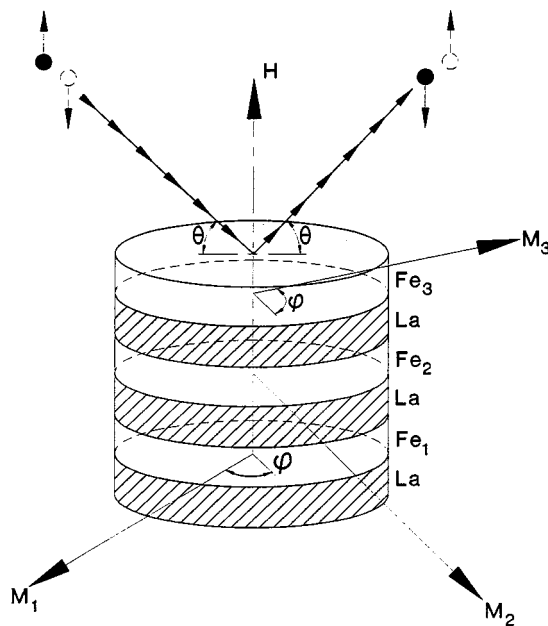


FIG. 6. An imprinted spiral magnetic structure and the neutron scattering configuration needed to ascertain its chirality (from Ref. 30).

surfaces and interfaces usually show some kind of imperfection. This could be interdiffusion (Fig. 7, left-hand side). Here, on an atomic scale, the lateral translational symmetry is broken. In the case of surface roughness (Fig. 7, center) the lateral correlation length could extend to thousands of angstroms. The two cases can be distinguished not by specular reflectivity—where it matters not just by the average scattering amplitude at each height z —but by diffuse scattering. The scattered beam Fig. 8 is defined by θ_f , the angle with the surface in the reflection plane, and φ , the angle off the reflection plane. Conservation of energy and momentum require that objects with an-plane repeat distance d_x , d_y are scattered with the law:

$$1/d_x = (1/\lambda)(\cos \theta_f \cos \varphi - \cos \theta_i), \tag{7}$$

$$1/d_y = (1/\lambda) \sin \varphi. \tag{8}$$

If $d_x = d_y$, the scattered beam in the reflection plane is much further away from the specular beam than the scattered beam off the reflection plane. Thus, it can be claimed³¹ that, by choosing the proper geometry, the scattering of particles ranging from tens of angstroms to tens of microns can be studied.

Roughness, and the off-specular scattering that it causes, has been extensively studied with x rays.³² Similar effects can take place in neutron scattering. For instance, neutron scattering has been observed of shear-induced ordering of dilute solutions of threadlike micelles;³³ not too dissimilar a figure of scattering may be obtained from lines of fluxoids

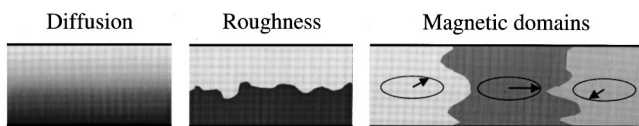


FIG. 7. Different types of breakdown of a layered structure.

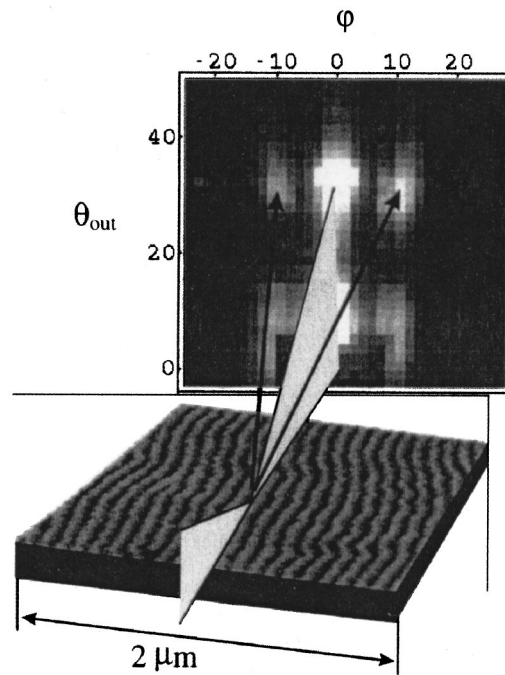


FIG. 8. Off-specular scattering from a network of magnetic domains in a $\text{Fe}_{0.5}\text{Pd}_{0.5}$ thin film. The top image is the scattering image as appearing in a position sensitive detector. The bottom image is a magnetic force microscope image of the magnetic domains; from Ref. 31.

parallel to the surface. In other cases lateral imperfections of magnetic origin have a flavor of their own. For instance in Fig. 7 (right-hand side) is presented in the case in which one layer of ferromagnet has been laterally subdivided in domains. Similar formation of lateral domains may take place in AF layers, and it has been actually observed in AF multilayers of Fe/Cr and similar materials.¹ It was easy to identify the origin of the diffuse scattering, because this appears as wings of the AF Bragg diffraction peak, but is totally absent from the structural Bragg peaks. Later work attempted to link the diffuse scattering AF scattering in Fe/Cr with the transport properties, including magnetoresistance, of multilayers annealed at different temperatures.³⁴ Recently the weak magnetic coupling in Co/Cu multilayers has been seen to give rise to domains with strong antiferromagnetic correlation between layers. These are present in the freshly prepared samples, but at the coercive field the domains within each cobalt layer loose (irreversibly) all correlations with the adjacent layers.³⁵ This evolution of the magnetic structure explains the observed decrease of the magnetoresistance from the virgin to the trained state. In yet another experiment on Fe/Cr multilayers an accurate analysis has been made of the shape of the AF diffuse scattering, as a result of model distributions of domains.³⁶

Surface magnetic structures have been studied by means of grazing incidence, large angle diffraction. If incident and exit angles θ_i and θ_f are below the critical angle for total reflection, then the penetration depth of the neutron evanescent wave below the sample surface is limited to 50–100 Å for most materials.³⁷ Intensity measured by scanning φ through a surface-plane Bragg reflection then arises solely from atoms confined to this thin surface layer. Even if the

neutrons are initially unpolarized, the diffracted intensities I^{++} and I^{--} appear at different spots, because within the ferromagnetic material, neutrons of opposite spin are refracted at different angles. An experiment run on the (110) surface Bragg peak of a fully magnetized Fe(100) film gave an unexpected result.³⁸ Aside from separated I^{++} and I^{--} intensities, different lobes indicated the presence of nonnegligible I^{+-} and I^{-+} , as if some of the magnetic moments of Fe were oriented perpendicular to the surface, possibly in a partially oxidized layer. Sensitivity to surface-normal magnetic components and to atomic order (inaccessible to specular reflectivity measurements), as well as depth resolution, are compelling advantages of grazing-angle diffraction which may overcome the difficulties of such technique.

We have seen how specular reflectivity of polarized neutrons has been applied to a broad range of magnetic problems, successfully solving some, while for others greater resolution and/or sensitivity is required. An order of magnitude improvement in dynamic range over current instruments would make possible the resolution of atom-scale structures. One could then measure the full spectrum of sample lengths from thousands of angstroms to interatomic spacings in a single specular measurement. Higher fluxes will also allow new ventures, such as the study of the kinetics and dynamics of the magnetization process. Finally, new applications will come with the construction and fabrication of novel magnetic systems, such as arrays of magnetic dots. The next decade will see technical developments that will come close to fulfilling those conditions. A new generation of high-flux pulsed neutron sources, as well as improvements in the optical components, will increase the useful neutron flux possibly by two orders of magnitude. In addition, the full utilization of three-dimensional neutron spin analysis and off-specular scattering may become possible common ground is established between experimental and theoretical efforts.

ACKNOWLEDGMENTS

This work was supported by the Department of Energy U.S. Office of Science-Material Sciences Contract No. 31-109-ENG-38. The author is grateful to C. Fermon, F. Givord, and E. Fullerton for giving permission to reproduce their figures, and to S.G.E. te Velthuis for a critical reading of the manuscript.

¹G. P. Felcher, *Physica B* **192**, 137 (1993); C. F. Majkrzak, *ibid.* **213**, 904 (1995); J. A. C. Bland, *ibid.* **234**, 458 (1997); G. P. Felcher, *ibid.* **267**, 154 (1999).

²A. G. Klein and S. A. Werner, *Rep. Prog. Phys.* **46**, 259 (1983).

³J. Lekner, *Theory of Reflection* (Nijhoff/Kluwer, Amsterdam, 1987).

⁴S. G. E. te Velthuis, G. P. Felcher, J. S. Jiang, A. Inomata, C. S. Nelson, A. Berger, and S. D. Bader, *Appl. Phys. Lett.* **75**, 4174 (1999).

⁵M. Tolan, *X-Ray Scattering from Soft-Matter Thin Films, Springer Tracts in Modern Physics* (Springer, Berlin, 1998), Vol. 148.

⁶X. L. Zhou and S. H. Chen, *Phys. Rep.* **257**, 223 (1995).

⁷J. Kasper, H. Leeb, and R. Lipperheide, *Phys. Rev. Lett.* **80**, 2614 (1998).

⁸C. F. Majkrzak and N. F. Berk, *Phys. Rev. B* **58**, 15416 (1998).

⁹G. P. Felcher, R. O. Hilleke, R. K. Crawford, J. Haumann, R. Kleb, and G. Ostrowski, *Rev. Sci. Instrum.* **58**, 609 (1987).

¹⁰S. J. Blundell and J. A. C. Bland, *Phys. Rev. B* **46**, 3391 (1992).

¹¹G. P. Felcher, R. T. Kampwirth, K. E. Gray, and R. Felici, *Phys. Rev. Lett.* **52**, 1539 (1984).

¹²H. Zhang, J. W. Lynn, C. F. Majkrzak, S. K. Satija, J. H. Kang, and X. D. Wu, *Phys. Rev. B* **52**, 10395 (1995).

¹³K. E. Gray, G. P. Felcher, R. T. Kampwirth, and R. Hilleke, *Phys. Rev. B* **42**, 3971 (1990).

¹⁴A. Mansour, R. O. Hilleke, G. P. Felcher, R. B. Laibowitz, P. Chaudhari, and S. S. P. Parkin, *Physica B* **156**, 867 (1989).

¹⁵J. M. Reynolds, V. Nunez, A. T. Boothroyd, T. Fretolft, D. G. Bucknall, and J. Penfold, *Physica B* **248**, 163 (1998).

¹⁶V. Lauter-Pasyuk, H. J. Lauter, M. Lorenz, V. L. Aksenov, and P. Leiderer, *Physica B* **267**, 149 (1999).

¹⁷S. W. Han, J. F. Ankner, H. Kaiser, P. F. Miceli, E. Paraoanu, and L. H. Greene, *Phys. Rev. B* **59**, 14692 (1999).

¹⁸S. M. Yusuf, E. E. Fullerton, R. M. Osgood, and G. P. Felcher, *J. Appl. Phys.* **83**, 6801 (1998).

¹⁹J. A. C. Bland, C. Daboo, B. Heinrich, Z. Celinski, and R. D. Bateson, *Phys. Rev. B* **51**, 258 (1995).

²⁰S. Hope, J. Lee, P. Rosdenbusch, G. Lauhoff, J. A. C. Bland, A. Ercole, D. Bucknall, J. Penfold, H. J. Lauter, V. Lauter, and R. Cubitt, *Phys. Rev. B* **55**, 11422 (1997).

²¹A. Barthelemy, A. Fert, M. N. Baibich, S. Hadjoudj, F. Petroff, P. Etienne, R. Cabanel, S. Lequien, F. Nguyen van Dau, and G. Creuzet, *J. Appl. Phys.* **67**, 5908 (1990).

²²F. Klose, C. Rehm, D. Nagengast, H. Maletta, and A. Weidinger, *Phys. Rev. Lett.* **78**, 1150 (1997).

²³B. Hjörvarsson, J. A. Dura, P. Isberg, T. Watanabe, T. J. Udovic, G. Andersson, and C. F. Majkrzak, *Phys. Rev. Lett.* **79**, 901 (1997).

²⁴C. F. Majkrzak, J. Kwo, M. Hong, Y. Yafet, D. Gibbs, C. L. Chien, and J. Bohr, *Adv. Phys.* **40**, 99 (1991).

²⁵E. E. Fullerton, S. Adenwalla, G. P. Felcher, K. T. Riggs, C. H. Sowers, S. D. Bader, and J. L. Robertson, *Physica B* **221**, 370 (1996).

²⁶A. Schreyer, J. F. Ankner, T. Zeidler, H. Zabel, M. Schäfer, J. A. Wolf, P. Grunberg, and C. F. Majkrzak, *Phys. Rev. B* **52**, 16066 (1995).

²⁷S. Adenwalla, G. P. Felcher, E. E. Fullerton, and S. D. Bader, *Phys. Rev. B* **53**, 2474 (1996).

²⁸J. G. LePage and R. E. Camley, *Phys. Rev. Lett.* **65**, 1152 (1990).

²⁹F. H. McGrath, N. Ryzhanova, C. Lacroix, D. Givord, C. Fermon, C. Miramond, G. Saux, S. Young, and A. Vedyayev, *Phys. Rev. B* **54**, 6088 (1996).

³⁰W. Lohstroh, M. Münzenberg, W. Felsch, H. Fritzsche, H. Maletta, R. Goyette, and G. P. Felcher, *J. Appl. Phys.* **85**, 5873 (1999).

³¹C. Fermon, F. Ott, B. Gilles, A. Marty, A. Menelle, Y. Samson, G. Legoff, and G. Francinet, *Physica B* **267–268**, 162 (1999).

³²S. K. Sinha, E. B. Sirota, S. Garoff, and H. B. Stanley, *Phys. Rev. B* **38**, 2297 (1988).

³³W. A. Hamilton, P. D. Butler, J. B. Hayter, L. J. Magid, and P. J. Kreke, *Physica B* **221**, 309 (1996).

³⁴W. Hahn, M. Loewenhaupt, G. P. Felcher, Y. Y. Huang, and S. S. P. Parkin, *J. Appl. Phys.* **75**, 3564 (1994).

³⁵J. A. Borchers, J. A. Dura, J. Unguris, D. Tulchinsky, M. H. Kelley, C. F. Majkrzak, S. Y. Hsu, R. Loloee, W. P. Pratt, Jr., and J. Bass, *Phys. Rev. Lett.* **82**, 2796 (1999).

³⁶Y. Endoh, M. Takeda, A. Kamijo, J. Mizuki, N. Hosoi, and T. Shinjo, *Mater. Sci. Eng.*, **B 31**, 57 (1995).

³⁷H. Dosch, B. W. Batterman, and D. C. Wack, *Phys. Rev. Lett.* **56**, 1144 (1986).

³⁸R. Günther, W. Donner, B. Toperverg, and H. Dosch, *Phys. Rev. Lett.* **81**, 116 (1998).